УДК 548:514:669

Crystal geometry of defectless three component $L2_1$ superstructure for antiphase boundaries specification in Heusler type compounds

Кристаллогеометрия бездефектной трехкомпонентной сверхструктуры $L2_1$ для определения спектра антифазных границ в сплавах Гейслера

E. A. Sharapov [1], E. A. Korznikova [2], A. S. Semenov [3], S. V. Dmitriev [4]
Е. А. Шарапов [1], Е. А. Корзникова [2], А. С. Семенов [3], С. В. Дмитриев [4]

[1] LLC Bashneft Polyus, Marx Str. 56, Ufa, 450015, Russia
[2, 4] Institute for Metals Superplasticity Problems of the Russian Academy of Sciences, Khalturin str. 39, Ufa, 450001, Russia
[3] North-Eastern Federal University, Polytechnic Institute (branch) in Mirny, Sakha (Yakutia), Tikhonov str. 5, building 1, Mirny, 678170, Russia
[2] elena.a.korznikova@gmail.com

[1] ООО «Башнефть Полюс», Россия, 450015, Уфа, ул. К. Маркса, 56
[2, 4] Институт проблем сверхпластичности металлов Российской академии наук, Россия, 450001, Уфа, ул. С. Халтурина, 39
[3] Северо-Восточный федеральный университет, Политехнический институт (филиал) в г. Мирный, Россия, 678170, Мирный, ул. Тихонова, 5, корп. 1
[2] elena.a.korznikova@gmail.com

ABSTRACT

Among the wide variety of ternary alloys, a special place is occupied by the group of Heusler compounds which are usually defined as ternary intermetallic compounds formed upon stoichiometric composition of A_2BC with $L2_1$ structure type. These materials demonstrate a set of unusual phenomena such as, for instance barocalorimetric, thermomagnetic effects, Peltier and Seebeck effects, shape memory effects and some others. Due to these unique properties Heusler compounds can be referred as a relevant object of investigation in modern material science community. It is well known, that in most cases properties of the material and its behaviour upon the modification of external conditions is defined by the defects present in the crystal lattice. The number of possible defect types grows upon the increase of the number of components and decrease of the crystal lattice symmetry class. In ordering alloys with complex internal structure and rigorous stoichiometry so called antiphase boundaries play a great role in the formation of the complex of properties of the material. In order to develop the classification of this defect type in frames of their geometrical and energetical characteristics for a definite superstructure one should carefully describe the crystallogeometry of the alloy considering the interactions in closest coordination spheres. The present work addresses the geometrical analysis of the Heusler compound type structure with A_2BC stoichiometry and $L2_1$ superstructure.

KEYWORDS

Crystal structure; intermetallic alloys; antiphase boundaries; Heusler alloys.

АННОТАЦИЯ

Среди большого разнообразия тройных сплавов особое место занимает группа сплавов Гейслера, которые обычно определяются как тройные интерметаллические соединения, образующиеся при стехиометрическом составе A_2BC с типом структуры $L2_1$. Эти материалы демонстрируют набор необычных явлений, как, например, барокалориметрический, термомагнитный эффекты, эффекты Пельтье, Зеебека, эффекты памяти формы и некоторые другие. Благодаря этим уникальным свойствам сплавы Гейслера могут быть отнесены к числу актуальных объектов исследования в современном материаловедении. Хорошо известно, что в большинстве случаев свойства материала и его поведение при воздействии внешних факторов определяется дефектами, присутствующими в кристаллической решетке. Количество возможных типов дефектов растет по мере увеличения количества компонентов и уменьшения класса симметрии кристаллической решетки. При анализе сплавов со сложной внутренней структурой строгая стехиометрия так называемых противофазных границ играет большую роль в формировании комплекса свойств материала. Для того чтобы разработать классификацию данного вида дефектов в рамках их геометрических и энергетических характеристик для определенной стехиометрии следует тщательно описать кристаллогеометрию сплава с учетом взаимодействий в ближайших координационных сферах. Настоящая работа посвящена геометрическому анализу системы Гейслера структура сложного типа со стехиометрией A_2BC и сверхструктурой $L2_1$.

КЛЮЧЕВЫЕ СЛОВА

Кристаллическая структура; интерметаллические сплавы; противофазные границы; сплавы Гейслера.

Introduction

Heusler and half-Heusler alloys have gained a considerable attention of researches due to their uniaue properties. Thus, the majority of shape memory magnetic alloys belong to Heusler alloy family. These are alloys based on Ni (and several based on Co) having an austenitic cubic phase with a superstructure $L2_1$ at high temperatures and low symmetry phase at low temperatures, which arises as a result of martensitic transformation [1–4].

Martensitic transformations are responsible for the exhibition of mechano-caloric effect, consisting in cooling the sample, subjected to uniaxial deformation (elastocaloric effect) or volumetric deformation (barocaloric effect) [2, 5–9]. Heusler Alloys exhibit Seebeck thermoelectric effects (the appearance of electric current in the presence of a temperature gradient in a thermoelectric material) and Peltier (cooling or heating of the sides of the material when passing electric current) [10–14]. The magnetocaloric effect is called change in temperature of a magnet as a result of release or absorption heat during cyclic exposure of a magnetic field to a substance. Some rare earth Heusler alloys exhibit very strong magnetocaloric effect, which creates real prerequisites for development based on them magnetic refrigeration devices, effectively operating in predetermined temperature ranges [15–17].

The physical and mechanical properties of Heusler type alloys are considerably affected by the lattice defects. Beside point defects, dislocations and grain boundaries the ordered alloys reveal another type of defects - antiphase boundaries associated with their superstructure and its violations. Antiphase boundaries in ordered alloys have been extensively studied by the group of prof. Starostenkov [18–21] where their evolution upon external impact and importance in frames of physical properties modification has been addressed.

This work presents the analysis of the crystal geometry of the Heusler type model compound with A_2BC stoichiometry that is required for addressing all possible types of antiphase defects in $L2_1$ superstructure.

1. Crystallography of defect-free superstructure $L2_1$

Representation of the superstructure $L2_1$ in the form of a union of shifts of 16 simple cubic lattices. Let us describe the packing of atoms in triple Heusler alloys of stoichiometric composition A_2BC with superstructure $L2_1$. As shown in fig. 2.1, this superstructure is a union of four fcc lattices, two of which are occupied by atoms of type A, one by atoms of type B, and one by atoms of type C. Each fcc lattice is a collection of four simple cubic lattices, that is, the superstructure $L2_1$ can be decomposed into 16 simple cubic gratings. Let us assume that the cubic translation cell shown in Fig. 1 in the Cartesian coordinate system xyz, has the lattice parameter a. It is convenient to conduct a crystal-geometric analysis of the superstructure by taking $a = 4$, in which case all atomic coordinates will be expressed as integers.

First of all, we define the lattice L as a set of points in three-dimensional space with radius vectors

$$\boldsymbol{x} = \mu_1 \boldsymbol{v}_1 + \mu_2 \boldsymbol{v}_2 + \mu_3 \boldsymbol{v}_3 , \qquad (1)$$

where μ_i – are any integers, $\boldsymbol{v}_i$ – are three linearly independent vectors that define the basis of the lattice.

Let the rows of the matrix V be the coordinates of the vectors $\boldsymbol{v}_i$ with respect to the Cartesian coordinate system xyz. Then the vector row of the coordinates of the vectors of the lattice L can be written in matrix form:

$$\boldsymbol{x} = \boldsymbol{\mu}\, V, \qquad (2)$$

where $\boldsymbol{\mu}$ – is a row vector of numbers μ_i. The matrix V is called the generating matrix of the lattice L, and vectors $\boldsymbol{v}_i$ – are called the generating vectors of this lattice. The primitive translation grid cell has a volume of $\det V$. We will number the generating vectors so that $\det V > 0$.

In the general case, the superstructure Q is defined as the union of the nodes $m = 1, 2, \ldots, M$ of the shifts of the lattice L, ascribing to each shift its own sort of atoms S_m, occupying the nodes of this shift:

$$Q = \bigcup_{m=1}^{M} (L + \boldsymbol{\mu}_m)_{Sm} . \qquad (3)$$

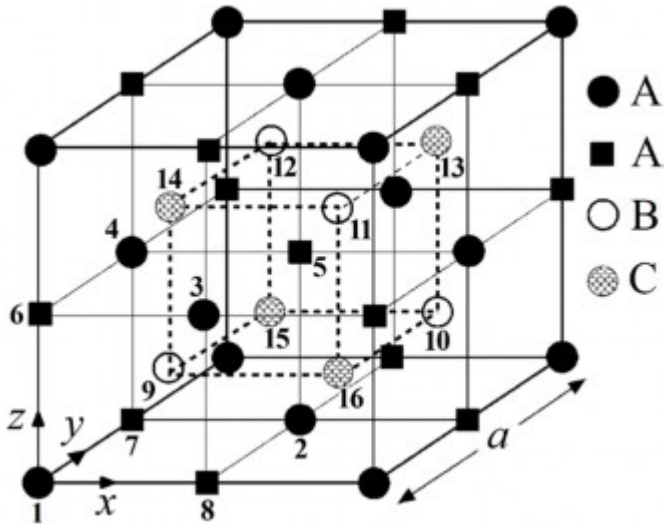

Fig. 1. The structure of the Heusler alloys of stoichiometric composition A_2BC with the lattice parameter *a*. The structure is composed of four nested fcc lattices or 16 nested simple cubic lattices (numbered). The cubic sublattices 1–11 are filled with atoms of type A, 9–12 atoms of type B, and 13–16 atoms of type C. If we neglect lattice distortions due to the difference in atom sizes, then we can assume that this superstructure is defined on a bcc lattice

Рис. 1. Структура сплавов Гейслера стехиометрического состава A_2BC с параметром решетки *a*. Структура состоит из четырех вложенных ГЦК-решеток или 16 вложенных простых кубических решеток (пронумерованных). Кубические подрешетки 1–11 заполнены атомами типа A, 9–12 атомами типа B и 13–16 атомами типа C. Если пренебречь искажениями решетки из-за разницы в размерах атомов, то можно предположить, что структура определена двумя вставленными друг в друга кубическими решетками

The superstructure $L2_1$ of A_2BC, stoichiometry, as noted above, can be represented as a combination of 16 shifts of a simple cubic lattice. We define a simple cubic lattice *L* with a lattice parameter equal to 4 generating vectors

$$\boldsymbol{\nu}_1 = (4,0,0),\ \boldsymbol{\nu}_2 = (0,4,0),\ \boldsymbol{\nu}_1 = (0,0,4). \quad (4)$$

The shear vectors in (3) will be defined as:

$$\begin{gathered}\boldsymbol{\mu}_1=(0,0,0),\ \boldsymbol{\mu}_2=(2,2,0),\ \boldsymbol{\mu}_3=(2,0,2),\ \boldsymbol{\mu}_4=(0,2,2),\\ \boldsymbol{\mu}_5=(2,2,2),\ \boldsymbol{\mu}_6=(0,0,2),\ \boldsymbol{\mu}_7=(0,2,0),\ \boldsymbol{\mu}_8=(2,0,0),\\ \boldsymbol{\mu}_9=(1,1,1),\ \boldsymbol{\mu}_{10}=(3,3,1),\ \boldsymbol{\mu}_{11}=(3,1,3),\ \boldsymbol{\mu}_{12}=(1,3,3),\\ \boldsymbol{\mu}_{13}=(3,3,3),\ \boldsymbol{\mu}_{14}=(1,1,3),\ \boldsymbol{\mu}_{15}=(1,3,1),\ \boldsymbol{\mu}_{16}=(3,1,1).\end{gathered} \quad (5)$$

Sorts of shears in (3) can be described as (see Fig. 1):

$$\begin{gathered}S_1=A,\ S_2=A,\ S_3=A,\ S_4=A,\\ S_5=A,\ S_6=A,\ S_7=A,\ S_8=A,\\ S_9=B,\ S_{10}=B,\ S_{11}=B,\ S_{12}=B,\\ S_{13}=C,\ S_{14}=C,\ S_{15}=C,\ S_{16}=C.\end{gathered} \quad (6)$$

Atom coordination in $L2_1$ superstructure. If we ignore the lattice distortions that arise during the relaxation of a structure containing three types of atoms, then we can approximately assume that the superstructure $L2_1$ is specified on the bcc lattice. It is known that atoms in cubic symmetry crystals are located relative to any selected atom on coordination spheres, which can be represented as a combination of the vertices of seven polyhedra (Fig. 2). The first two polyhedra - the octahedron and the cube, are two of the five bodies of Plato, all faces of which are the same. The remaining five polyhedra are the bodies of Archimedes. There are seven polyhedra because there are seven possible ratios of the node indices [[h, k, l]] in the cubic lattice, namely:

1. $|h|\neq|k|=|l|=0$, 6 vertex octahedron;
2. $|h|=|k|=|l|\neq0$, 8 vertex cube;
3. $|h|=|k|\neq|l|=0$,12 vertex kubooktaedr;
4. $|h|>|k|\neq|l|=0$,6 vertex octahedron;
5. $0\neq|h|<|k|=|l|$, 24 vertex truncated octahedron;
6. $|h|>|k|=|l|\neq0$, 24 vertex rhombocuboctahedron;
7. $|h|>|k|>|l|\neq0$, 48 vertex truncated cuboctahedron.

Considering each of the four atoms included in the primitive translation cell as the central one, we describe the filling of the coordination spheres with atoms of various sorts. This information is summarized in Table 1 where the example of filling of coordination spheres around an atom of the sort A is presented. The table indicate the number of the coordination sphere (up to and including the 14th), the radius of the coordination sphere, the total number of atoms on each sphere, and the number of atoms of each sort. In addition, a polyhedron (or polyhedra) is indicated at the vertices of which atoms are located on each of the coordination spheres.

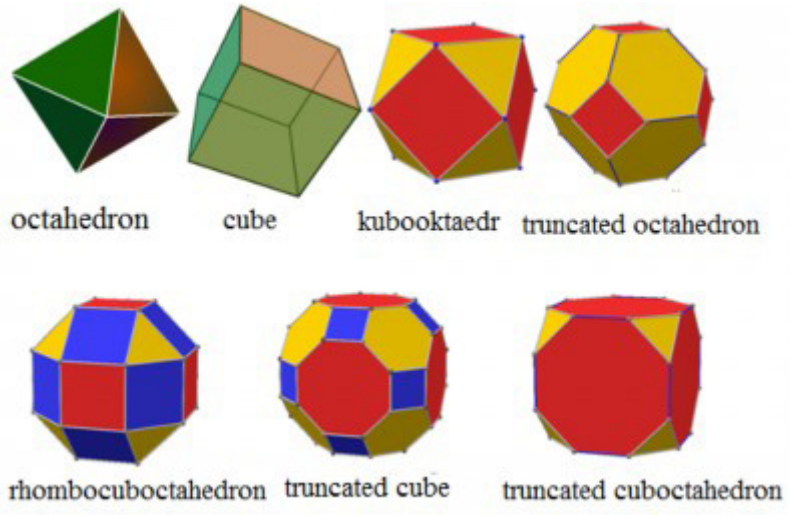

Fig. 2. Seven coordination polyhedra for cubic symmetry lattices and their abbreviations. Number of vertices: octahedron 6, cube 8, cuboctahedron 12, truncated octahedron 24, truncated cube 24, rhombocuboctahedron 24, truncated cuboctahedron 48. Images of polyhedra are adopted from Wikipedia

Рис. 2. Семь координационных многогранников для решеток кубической симметрии. Количество вершин в многогранниках: октаэдр – 6, куб – 8, кубоктаэдр – 12, усеченный октаэдр – 24, усеченный куб – 24, ромбокубооктаэдр – 24, усеченный кубоктаэдр – 48. Изображения многогранников адаптированы из Википедии

Table 1
Таблица 1

Filling of coordination spheres around an atom of the sort *A*

Заполнение координационных сфер вокруг атома рода *A*

Number of the coordination sphere	Radius of the coordination sphere	Number of atoms			
			A sort	*B* sort	*C* sort
1	4√3/a	8	0	4	4
2	4√4/a	6	6	0	0
3	4√8/a	12	12	0	0
4	4√11/a	24	0	12	12
5	4√12/a	8	8	0	0
6	4√16/a	6	6	0	0
7	4√19/a	24	0	12	12
8	4√20/a	24	24	0	0
9	4√24/a	24	24	0	0
10	4√27/a	32	0	16	16
11	4√32/a	12	12	0	0
12	4√35/a	48	0	24	24
13	4√36/a	30	30	0	0
14	4√40/a	24	24	0	0

The results obtained allow, on a qualitative level, to estimate the contributions of various pair bonds to the sublimation energy of the alloy. So, if we confine ourselves to the analysis of the environment of atoms in the first three coordination spheres, we can conclude that atoms of sort A on the first sphere of 8 neighbors have 4 atoms of type B and sort C. However, only atoms of type A are located on the second and third spheres in the amount of 6 and 12, respectively. In an atom of sort C, in the first sphere all 8 atoms are of sort A, in the second all 6 atoms of grade B, and in the third all 12 atoms of sort C. In an atom of grade B in the first sphere all 8 atoms are of sort A, in the second all 6 atoms sort C, and on the third all 12 atoms of sort B.

Conclusions

The conducted work resulted in the description of filling the coordination spheres with atoms of different sorts around atoms of types A, B, and C up to the 14th coordination sphere in $L2_1$ superstructure with A2BC stoichiometry. The results obtained allow, on a qualitative level, to judge the contributions of various pair bonds to the sublimation energy of the alloy.

We have also obtained the expression of the sublimation energy of the alloy through the energies of pair interactions that allows to conclude that in the first coordination sphere, only AB and AC bonds contribute to the sublimation energy. In the second sphere, the contribution from the bonds AA and BC appears. Relations between BB and CC only contribute from the 3rd coordination range.

The presented analysis allowed to obtain in the specification of all energetically equivalent but geometrically different representations of the $L2_1$superstructure which result from shifts by one of the lattice vectors, while the point symmetry transformations do not give new geometrically different representations of the $L2_1$ superstructure. This information is necessary for the classification of planar superstructural defects in Heusler alloys which in turn defines the structural features and related properties aspects. The detailed classification of superstructural antiphase boundaries based in the performed analysis will be addressed in subsequent publications of the authors.

Acknowledgments

KEA thanks for the financial support the Council of the President of the Russian Federation for state support of young Russian scientists, grant No MD-3639.2019.2. SAS is gratefully acknowledges the financial support of Russian foundation for Fundamental Research, grant No. 18-32-00171 mol_a.

References

1. Role of twin and anti-phase defects in MnAl permanent magnets / S. Bance et. al. // Acta Materialia. 2017. V. 131. P. 48–56. DOI:10.1016/j.actamat.2017.04.004.

2. Martensitic stabilization and defects induced by deformation in TiNi shape memory alloys / S. Wang et. al. // International Journal of Minerals, Metallurgy and Materials. 2011. V. 18. P. 66–69. DOI: 10.1007/s12613-011-0401-5.

3. Highly mobile twin boundaries in seven-layer modulated Ni–Mn–Ga–Fe martensite / A. Sozinov et. al. // Scripta Materialia. 2020. V. 178. P. 62–66. DOI: 10.1016/j.scriptamat.2019.10.042.

4. Heczko O. Antiphase boundaries in ni-mn-ga ordered compound // AIP Advances. 2020. V. 10. DOI: 10.1063/1.5130183.

5. Reducing mechanical hysteresis via tuning the microstructural orientations in Heusler-type Ni44.8Mn36.9In13.3Co5.0 elastocaloric alloys / B. Lu et. al. // Journal of Alloys and Compounds. 2019. V. 785. P. 1023–1029. DOI: 10.1016/j.jallcom.2019.01.276.

6. Czernuszewicz A., Kaleta J., Lewandowski D. Multicaloric effect: Toward a breakthrough in cooling technology // Energy Conversion and Management. 2018. V. 178. P. 335–342. DOI: 10.1016/j.enconman.2018.10.025.

7. Enhanced barocaloric effect produced by hydrostatic pressure-induced martensitic transformation for Ni44.6Co5.5Mn35.5In14.4 Heusler alloy / X. He et. al. // Scripta Materialia. 2018. V. 145. P. 58–61. DOI: 10.1016/j.scriptamat.2017.10.015.

8. A unified approach to describe the thermal and magnetic hysteresis in Heusler alloys / J. S. Blázquez et. al. // Appl. Phys. Lett. 2016. V. 109. P. 122410. DOI: 10.1063/1.4963319.

9. First-principles investigations of caloric effects in ferroic materials / P. Entel et. al. // AIP Conf. Proc. 2018. V. 1461. P. 11–23. Berhampur, Odisha, India. DOI: 10.1063/1.4736867.

10. Novel synthesis and processing effects on the figure of merit for NbCoSn, NbFeSb, and ZrNiSn based half-Heusler thermoelectrics / S. V. Pedersen et. al. // Journal of Solid State Chemistry. 2020. 121203. DOI:10.1016/j.jssc.2020.121203.

11. 2019 Effect of temperature dependent relaxation time of charge carriers on the thermoelectric properties of LiScX (X=C, Si, Ge) half-Heusler alloys / A. Saini et. al. // Journal of Alloys and Compounds. 2019. V. 806. P. 1536–1541. DOI: 10.1016/j.jallcom.2019.07.306.

12. Computational Nano-materials Design for Colossal Thermoelectric-cooling Power by Adiabatic Spin-Entropy Expansion in Nano-superstructures / H. Katayama-Yoshida et. al. // Jpn. J. Appl. Phys. 2007. V. 46. P. L777–L779. DOI: 10.1143/JJAP.46.L777.

13. Modeling and Sizing of a TEG with Half-Heusler TE Legs for Reducing Fuel Consumption in a Heavy Duty Vehicle / A. Contet et. al. // Conference: WCX SAE World Congress Experience. 2019. DOI: 10.4271/2019-01-0897.

14. Thermomagnetic properties of single crystal Ni54Fe19Ga27 Heusler alloys / V. Basso et. al. // Journal of Applied Physics. 2009. V. 105. P. 07A937. DOI: 10.1063/1.3073838.

15. 2019 The Characteristic Properties of Magnetostriction and Magneto-Volume Effects of Ni2MnGa-Type Ferromagnetic Heusler Alloys / T. Sakon et. al. // Materials. 2019. V. 12, No. 22. P. 3655. DOI: 10.3390/ma12223655.

16. Temperature dependent magnetostrains in polycrystalline magnetic shape memory Heusler alloys / V.A. Chernenko et. al. // Journal of Alloys and Compounds. 2013. V. 577. P. S305–S308. DOI: 10.1016/j.jallcom.2011.12.117.

17. Magnetocaloric Effect and Magnetostriction in a Ni49.3Mn40.4In10.3 Heusler Alloy in AC Magnetic Fields / L. N. Khanov et. al. // Phys. Solid State. 2018. V. 60. P. 1111–1114. DOI: 10.1134/S1063783418060148.

18. Starostenkov M. D., Chaplygina A. A., Chaplygin P. A. Influence of Antiphase Boundaries on Structural and Energy Characteristics of Alloy Cu3Pt5 // Inorg. Mater. Appl. Res. 2018. No. 9. P. 566–569. DOI: 10.1134/S207511331804038X.

19. Investigation of Growth Ordered Phases in the Alloy NiAl Equiatomic Composition During Stepwise Cooling / M. Starostenkov et. al. // Procedia IUTAM. 2017. V. 23. P. 78–83. DOI: 10.1016/j.piutam.2017.06.007.

20. Starostenkov M., Chaplygina A., Romanenko V. Details of the Formation of Superstructures in the Process of Ordering in Cu-Pt Alloys // KEM. 2013. V. 592–593. P. 321–324. DOI: 10.4028/www.scientific.net/KEM.592-593.321.

21. Investigation of Growth Ordered Phases in the Alloy NiAl Equiatomic Composition during Stepwise Cooling / M. Starostenkov et. al. // Iutam Symposium On Growing Solids. 2017. V. 5. P. 78–83. DOI: 10.1016/j.piutam.2017.06.007.